

led, in some cases, to gravity-differentiated layered complexes; (iii) emplacement of ultramafic rocks, either as plastic crystalline mushes or as serpentized masses; and (iv) hydrothermal metamorphism of the fresh mafic and ultramafic rocks, involving a volume increase. The relative importance of these processes appears to differ from one oceanic ridge to another.

WILLIAM G. MELSON

Smithsonian Institution,
Washington, D.C. 20560

GEOFFREY THOMPSON

Woods Hole Oceanographic
Institution, Woods Hole,
Massachusetts 02543

References and Notes

1. J. R. Cann and B. Funnel, *Nature* **217**, 661 (1967).
2. The analyzed sample (AII 20-Dr 16-46) has been entered in the collection of the U.S. National Museum under number 110753/46.
3. L. R. Wager and W. A. Deer, *Medd. Gronland* **105**, 1 (1939).
4. H. H. Hess, *The Stillwater Igneous Complex, Montana* (Geological Society of America, New York, 1960).
5. A comprehensive review of continental layered intrusions, including grain size characteristics, has been recently compiled by L. R. Wager and G. M. Brown, *Layered Igneous Rocks* (Freeman, San Francisco, 1968).
6. The "oceanic tholeiites" of A. E. J. Engel, C. G. Engel, R. G. Havens [*Geol. Soc. Amer. Bull.* **76**, 719 (1965)].
7. C. G. Engel and R. L. Fisher, *Science* **166**, 1136 (1969).
8. F. Aumento, *ibid.* **165**, 1112 (1969).
9. T. P. Thayer, *Geol. Soc. Amer. Bull.* **80**, 1515 (1969).
10. I. D. Muir and C. E. Tilley, *J. Petrology* **5**, 409 (1964).
11. E. Bonatti, *Nature* **219**, 363 (1968).
12. F. J. Vine, *Science* **154**, 1405 (1966).
13. For a discussion of geophysical models of the oceanic crust see X. Le Pichon, *Tectonophysics* **7**, 385 (1969).
14. For example, St. Paul's Rocks, equatorial Atlantic [W. G. Melson, E. Jarosewich, V. T. Bowen, G. Thompson, *Science* **155**, 1532 (1967)]; mid-Atlantic Ridge, 43°N [J. D. Phillips, G. Thompson, R. P. Von Herzen, V. T. Bowen, *J. Geophys. Res.* **74**, 3069 (1969)]; Vema Fracture, 11°N [W. G. Melson and G. Thompson, *Trans. Roy. Soc. London*, in press].
15. Yu. A. Bogdanov and V. V. Ploshko, *Dokl. Akad. Nauk SSSR* **177**, 173 (1968).
16. J. R. Cann, *J. Petrology* **10**, 1 (1969).
17. R. L. Fisher and C. G. Engel, *Geol. Soc. Amer. Bull.* **80**, 1373 (1969).
18. R. L. Fisher, C. G. Engel, T. W. C. Hilde, *Deep-Sea Res.* **15**, 521 (1968).
19. W. G. Melson, E. Jarosewich, R. Cifelli, G. Thompson, *Nature* **215**, 381 (1967).
20. W. G. Melson, G. Thompson, Tj. H. van Andel, *J. Geophys. Res.* **73**, 5925 (1968).
21. I. D. Muir and C. E. Tilley, *J. Petrology* **7**, 193 (1966).
22. S. H. Quon and E. G. Ehlers, *Geol. Soc. Amer. Bull.* **74**, 1 (1963).
23. J. D. H. Wiseman, *Sci. Rep. John Murray Exped. Brit. Mus. (Natur. Hist.)* **3**, 1 (1937).
24. K. Yagi, *Proc. Jap. Acad.* **36**, 213 (1960).
25. G. Thompson and D. C. Bankston, *Spectrochim. Acta Part B* **24**, 335 (1969).
26. We thank the officers, crew, and scientists of cruises 20 and 42 of R. V. *Atlantis II*; Dr. V. T. Bowen, who organized the sampling program and reviewed the manuscript; and Dr. T. Simkin of the Smithsonian Institution, who also critically reviewed the manuscript. This work was supported by the U.S. Atomic Energy Commission under contract AT(30-1)-2174 with the Woods Hole Oceanographic Institution, and by Smithsonian Research grants. Contribution 2469 of the Woods Hole Oceanographic Institution.

2 February 1970; revised 2 April 1970

Filamentary Crystal Growth Associated with Impact Craters from Hypervelocity Microparticles

Abstract. *A filamentary crystal growth is associated with impacts of hypervelocity microparticles upon copper foil. They are copper whiskers formed by the condensation of the target material vaporized by the impact.*

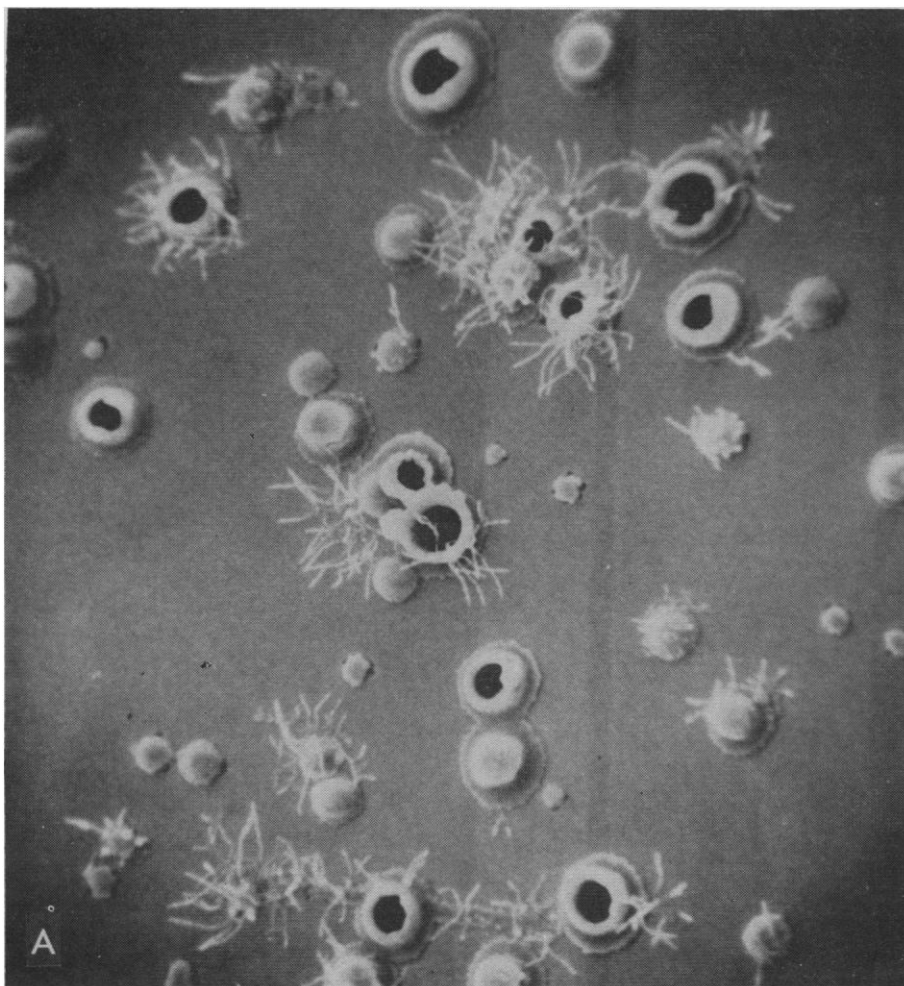
Filamentary crystalline growth is observed in the immediate area of impact sites of hypervelocity microparticles upon thin copper foil. Carbonyl iron spheres, ranging in diameter from 0.05 to 5 μm , were accelerated in an electrostatic accelerator to velocities of 1.5 to 50 km/sec and impinged upon rolled copper foil 3 μm thick. The impacts occurred while the thin film was at room temperatures at a pressure of 5×10^{-5} torr.

Portions of the exit side of the foil were photographed with a Cambridge scanning electron microscope (Fig. 1, A to C). Approximately 27 percent of the projectiles penetrated the foil as shown. Unfortunately, neither particle velocity nor particle size can be correlated with any specific impact sites shown. However, from past studies of craters produced in thin films by hyper-

velocity microparticles it is safe to assume that the successful penetrations and the larger impact areas were caused by the larger and consequently slower particles.

Several interesting features concerning the filamentary crystalline growth are revealed by the photographs of the exit side of the foil (the filamentary phenomenon does not appear on the impact side of the foil).

1) The filaments exhibit great strength. The average diameter of the "stem" between the nodules is about 0.2 μm , whereas the overall filamentary length often exceeds 12 μm . This structure survived repeated exposures to vacuum and atmospheric pressure and to ambulatory transportation between buildings. There is a noticeable absence of broken or separated filaments lying on the surface.



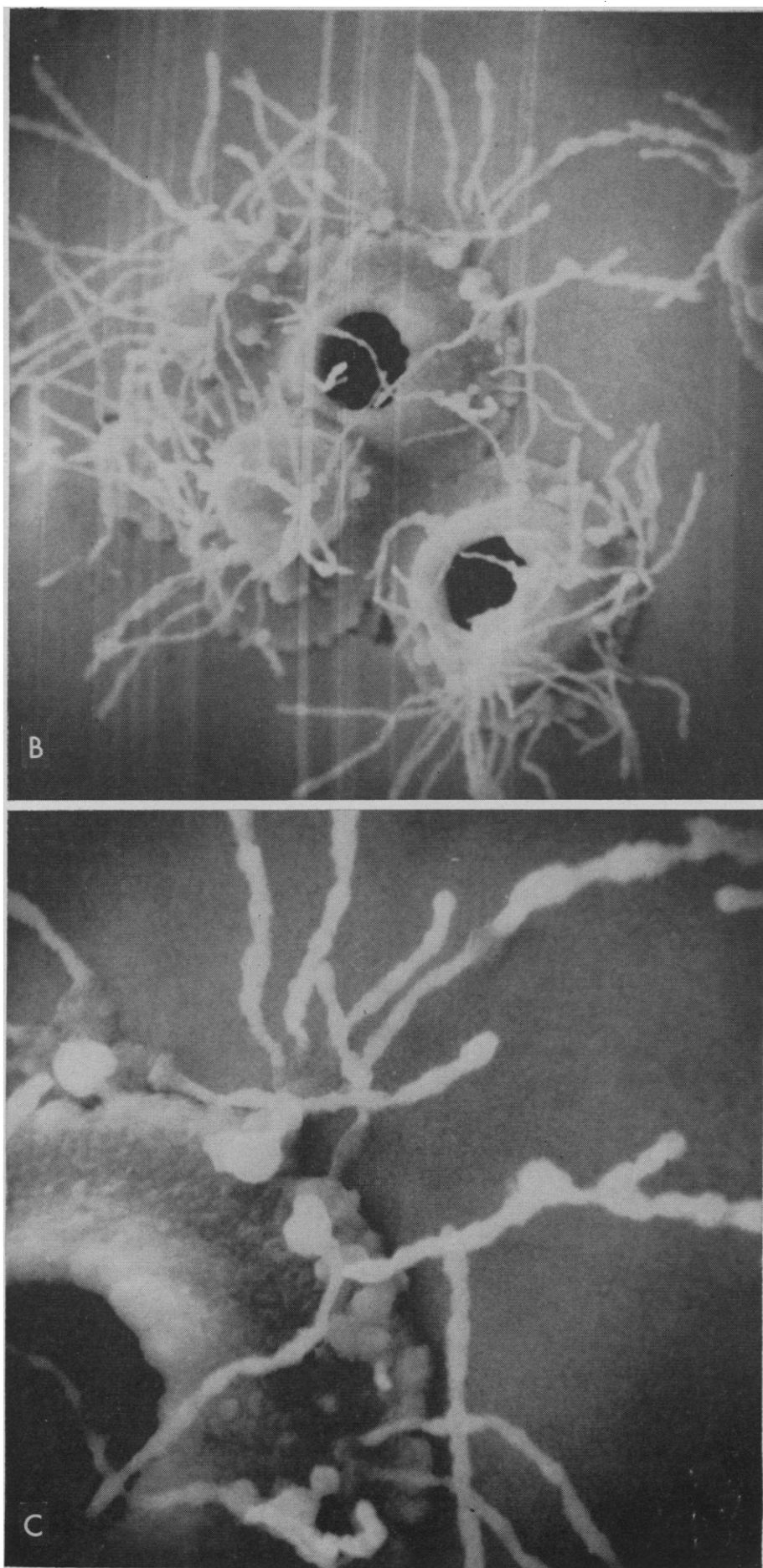


Fig. 1. Exit side of copper foil. (A) Magnified $\times 920$; (B) magnified $\times 3440$; and (C) magnified $\times 8900$.

2) The filaments appear on several of the impact areas which do not show penetration. This observation essentially rules out interaction between the iron in the projectile and the copper metal.

3) Some of the filaments are branched, which indicates a "relatively slow growth" or formation as opposed to violent formation by ejecta or high temperature spewing or extrusion.

4) The nodules in the filaments are similar to the structure surrounding the perforations (Fig. 1C).

The following conclusions are based upon a study of the photographs shown and considerations of physical phenomena normally associated with the impact of hypervelocity microparticles. The strength exhibited by the filaments suggests single crystals of copper or copper whiskers formed by the condensation of copper vapor surrounding the exit side of the impact site. The elastic limit and tensile strength of whiskers are "100 to 1000 times greater than that of the annealed bulk crystal" (1). The extremely high pressure and temperature conditions prevalent during impact are highly favorable toward the formation of copper vapor, and the low-pressure volume surrounding the foil and the impact site are similarly highly favorable toward condensation of the copper vapor after impact. Pressures as high as 12 megabars develop in 0.017×10^{-9} second in a volume of the target immediately below the impact site (2). Less than a nanosecond later, this high-pressure volume of copper erupts on the exit side of the foil into the ambient vacuum chamber pressure of 5×10^{-6} torr, and condensation occurs.

The absence of whiskers on the impact side of the foil is probably due to the fact that the ultra-high-speed ejecta or secondary spray normally associated with the impact side of the hypervelocity particle impact site removed the copper vapor too quickly for localized condensation. The absence of whiskers on the exit side of some of the impacts is not readily explained except that conditions for the formation of whiskers are probably quite critical and that those conditions did not necessarily prevail at all the impact sites.

The whiskers may have been products of high-impact, plastic deformation of individual copper crystals in the rolled foil. However, the propagation of the whiskers along the flaw line and the "branched" filaments tend

to negate such an explanation. Similar crystalline growth has been observed on electrodes following studies of exploding wire (3). In this type of experiment, a copper wire, supported between two large electrodes, is subjected to a high current, fast-rise pulse and "exploded," producing hypervelocity copper fragments (and copper vapor).

No analytical studies of the composition of the whiskers were made. Several repeated attempts at reproducing the phenomenon have met with limited success in that the whiskers are considerably shorter and of a larger diameter. If attempts to reproduce longer crystals succeed, composition and better correlation of projectile size and velocity and the filamentary growth may be determined.

OTTO E. BERG

J. A. M. McDONNELL*

Theoretical Studies Branch,
Goddard Space Flight Center,
Greenbelt, Maryland 20771

References and Notes

1. S. S. Brenner, *Properties of Whiskers in Growth and Perfection of Crystals*, R. H. Doremus, B. W. Roberts, D. Turnbull, Eds. (Wiley, New York, 1958), p. 161.
2. B. A. Sodek, thesis, Oklahoma State University (1966).
3. J. L. Bohn, personal communication.
4. We thank R. Anstead (NASA) for electron microscopy.

* Present address: Department of Physical Electronics, University of Kent, Canterbury, England.

16 March 1970

Pleistocene Paleotemperatures

Abstract. *The generalized isotopic paleotemperature curve reproduces absolute temperatures to within 1°C; it closely reflects faunal changes; and its time scale is correct to within a very few percent back to at least 175,000 years. The average oxygen isotopic composition of the North American and European ice caps was about -9 per mil.*

The generalized paleotemperature curve (Fig. 1), based on oxygen isotopic analysis of planktonic Foraminifera from deep-sea cores, was proposed in 1955 (1), and extended in 1966 (2), as a representation of surface temperatures at low latitudes in the Atlantic Ocean and adjacent seas during the past 425,000 years.

Some authors have maintained that this curve is not in accord with the foraminiferal evidence (3, 4); that it represents not temperatures but, largely or even totally, isotopic variations of the seawater (5-7); and that its time

scale is not accurate but should be stretched by 25 percent (8, 9). The purpose of the present report is to review the evidence upon which these contentions are based and to demonstrate the validity of the curve as originally proposed. In the process, a close estimate is derived for the average oxygen isotopic composition of the North American and European ice caps.

The contention that the foraminiferal evidence is not in accord with the isotopic evidence stems solely from Ericson and Wollin's choice of *Globorotalia menardii* as the best temperature indicator and from the artificial boundary condition that they used in estimating the foraminiferal abundances (10). *Globorotalia menardii* is a highly polytypic species which produced at least three distinct subspecies during the past 425,000 years, each having different temperature tolerances (11, 12). On the basis of the choice of this species as the best temperature indicator, core layers in which *G. menardii* is absent but other species even more restricted to warm waters (*Pulleniatina obliquiloculata*, *Sphaeroidinella dehiscens*) are abundant have been consistently defined as "cold" and presented as an example of discordance between evidence derived from isotopes and that derived from micropaleontology. By labeling this species as "very abundant" if more than "100 specimens per tray spread" were noticed (10), Ericson and Wollin saw none of the abundance variations above the "100 specimens per tray spread" level; this resulted in published "climatic" curves [for example, figure 3 in (3); figure 2 in (13)] containing only a vastly truncated portion of the available evidence (blackened section of Fig. 2B). It is upon these truncated curves that a "climatic" curve claimed to represent the entire Pleistocene has been constructed [figure 5 in (13)].

The artificial boundary condition mentioned restricts the application of Ericson and Wollin's visual method to those foraminiferal species whose abundances range from 0 to 100 specimens per tray spread. In these cases (Fig. 3C) a good correlation with the paleo-

temperature curve (Fig. 3A) is observed. An even better correlation is obtained if ratios of warm to cold species are used because the temperature signal is thus amplified (Fig. 3B).

Using accurate countings (516 specimens or more) instead of visual appreciation, Lidz (14) studied in detail foraminiferal abundances in a long and undisturbed deep-sea core from the Caribbean. His results (Fig. 4, A through I) show such a close relationship with the isotopic curve (Fig. 4J) that the foraminiferal abundance curves can be used in lieu of the isotopic curve for both temperature estimates and spectral analysis. An intimate relationship between isotopic temperature and foraminiferal parameters has also been found by Imbrie (15), who used factor analysis on different latitudinal assemblages, and by Ruddiman (16), who used the net excess of warm or cold species (Fig. 5). Finally, I demonstrated the excellent relationship between major and minor isotopic temperature variations and shell morphology of monospecific populations of pelagic Foraminifera (11).

It is apparent that all foraminiferal evidence now available, including the evidence provided by Ericson and Wollin (3, 4, 10) if the artificial boundary condition mentioned above is eliminated, is in complete agreement, usually down to minor details, with the results obtained by the application of Urey's method of paleotemperature analysis to pelagic Foraminifera from deep-sea cores. Anyone wishing to question this conclusion must first demolish all foraminiferal evidence mentioned above.

The glacial/interglacial range of the O^{18}/O^{16} composition of planktonic Foraminifera of shallow habitat (*Globigerinoides sacculifera* and *G. rubra*) from Caribbean and equatorial Atlantic deep-sea cores is 1.8 per mil for the more recent temperature stages (stages 1 to 6) and decreases to 1.6 per mil for the earlier stages (2). This isotopic amplitude, if entirely due to temperature, would represent a glacial/interglacial temperature range of 7° to 8°C. However, a portion of this range [about 30

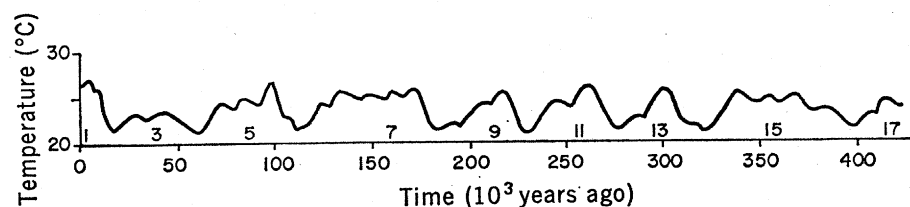


Fig. 1. Generalized paleotemperature curve (from 2). Odd integers above the abscissa identify warm temperature stages.